Determination of Volume Fractions of Texture Components with Standard Distributions in Euler Space

JAE-HYUNG CHO, A.D. ROLLETT, and K.H. OH

The intensities of texture components are modeled by Gaussian distribution functions in Euler space. The multiplicities depend on the relation between the texture component and the crystal and sample symmetry elements. Higher multiplicities are associated with higher maximum values in the orientation distribution function (ODF). The ODF generated by Gaussian function shows that the S component has a multiplicity of 1, the brass and copper components, 2, and the Goss and cube components, 4 in the cubic crystal and orthorhombic sample symmetry. Typical texture components were modeled using standard distributions in Euler space to calculate a discrete ODF, and their volume fractions were collected and verified against the volume used to generate the ODF. The volume fraction of a texture component that has a standard spherical distribution can be collected using the misorientation approach. The misorientation approach means integrating the volume-weighted intensity that is located within a specified cut-off misorientation angle from the ideal orientation. The volume fraction of a sharply peaked texture component can be collected exactly with a small cut-off value, but textures with broad distributions (large full-width at half-maximum (FWHM)) need a larger cut-off value. Larger cut-off values require Euler space to be partitioned between texture components in order to avoid overlapping regions. The misorientation approach can be used for texture's volume in Euler space in a general manner. Fiber texture is also modeled with Gaussian distribution, and it is produced by rotation of a crystal located at g_0, around a sample axis. The volume of fiber texture in wire drawing or extrusion also can be calculated easily in the unit triangle with the angle distance approach.

I. INTRODUCTION

A polycrystalline material consists of many crystals with different phases, shapes, sizes, and orientations. For this article, a single-phase, fully dense solid is assumed with uniform chemical composition. The orientations of the crystals or grains in a polycrystal are typically not randomly distributed after thermomechanical processing and the dominance of certain orientations may affect materials properties. The orientation distribution function (ODF, $f(g)$) in Euler space is the probability density of orientation in a polycrystalline material. The ODF has normalized positive values and there are two limiting cases, *i.e.,* the random distribution and single-crystal case. The former corresponds to $f(g) = 1$ and the latter is represented by a delta function, $f(g) = 8\pi^2\delta(g - g_0)$, where the orientations of all crystallites have the same orientation $g = g_0$. The summation over the ODF is unity by normalization. Quantitative texture analysis based on pole figures is a kernel problem, and several methods such as the series expansion, the WIMV, and the Vector methods, are used for the calculation of the ODF. The ODF is essential information for optimization of anisotropy and mechanical properties.[1–5] The WIMV with an automated conditional ghost correction suggested by Mathies and Vinel is the reproduction method of the ODF from pole figure. It is based on the analysis of the structure of the exact solution of the central problem, of the analytical properties of the ghosts problem and of the use of the most construcive elements of earlier reproduction activities by Williams and Imhof. With reference to these authors it bears the acronym WIMV.

Model distributions have been used for analyzing the reliability of mathematical reproduction methods of the ODF from pole figures and for investigating ghost effects. The Gauss-shaped distribution suggested by Bunge has been used widely in texture analysis.[6] This model can be represented by series in harmonic functions, but leads to termination errors. It can be calculated in a numerical form for small full-width at half-maximum (FWHM, b; $b << \pi$). The Gauss-shaped function proposed by Bunge is not symmetric about $\tilde{\omega} = \pi$, and the general property of the orientation distance, $\tilde{\omega} = \pi + \varepsilon \cong \pi - \varepsilon$ is not satisfied, where ε is a finite angle (orientation distance, $\tilde{\omega}$ is defined in Eqs. [5] through [7]). Matthies proposed a different standard function with a physically reasonable and mathematically simple form, which satisfies the property of orientation distance and is not limited to small FWHM.[7,8] This standard function has an analytically closed form and the values can be tabulated.

The development of the rolling textures in copper and α brass was studied with the help of Gauss model calculations.[9] This method was able to give a complete quantitative description of the main texture peaks and their dispersion with good approximation at high rolling reductions. The description of ODF by the superposition of Gauss-type model functions for the purpose of information condensation and ghost correction was considered and was found to be useful.[10] For both recrystallization and deformation textures, Gauss function models are also well suited for the presentation of ODF.

In order to describe an orientation, g, several mathematical parameters can be used. These include rotation or orientation matrices, Miller indices, Euler angles, angle/axis of rotation,

JAE-HYUNG CHO, Research Scholar, is with the Sibley School of Mechanical and Aerospace Engineering, Cornell University, Ithaca, NY 14853. Contact e-mail: kyuhwan@snu.ac.kr A.D. ROLLETT, Professor, is with the Materials Science and Engineering Department, Carnegie Mellon University, Pittsburgh, PA 15213-3890. K.H. OH, Professor, is with the Materials Science and Engineering Department, Seoul National University, Seoul, Korea 151-744.

Manuscript submitted September 11, 2002.

Rodrigues vectors, and unit quaternions. All of these are used for the description of different aspects of macrotexture and microtexture measurements.[11] The misorientation angle/axis between two texture components can be calculated easily. These values can be used as the useful characteristics of the different two orientations or crystals in polycrystalline materials.[12] Mackenzie and Handscomb calculated the misorientation distribution in a randomly oriented cubic material.[13,14] They showed that the average value of misorientation is located around 45 deg and the maximum is about 62.8 deg. Morawiec reported the distribution of misorientation angles and misorientation axes for crystallites with different symmetries.[15] The misorientation is also used for characterization of materials microtextures. Rajan and Petkie measured wire textures, for example, using electron backscatter diffraction and displayed the results with Rodrigues–Frank maps in addition to inverse pole figures and standard pole figures.[16] In order to calculate the average orientation within a grain, Barton and Dawson have used misorientation angles.[17] Many researchers have investigated methods of determining a suitable average orientation from a set of orientations.[18,19]

Texture components in real materials often have Gauss-shaped distributions as measured in a diffraction experiment. Gauss-shaped distributions have a bell shape with FWHM, *b,* and maximum at the ideal component, g_0. When considering the volume fractions of texture components, it is useful to define a window about g_0 based on a difference in orientation measured by misorientation angle between g_0 and its surrounding components. All of the ODFs, $f(g)$, within the acceptance angle can be assumed to be a part of the ideal texture component, g_0 and be added to the volume of component of g_0. The misorientation angle is a useful measure of distance from a component for the volume fraction calculation in ODF space.

When considering the ODF in orientation space, the volume element with metric is also important. Quantities such as an ODF described in a non-Euclidean space are distorted in some way that is specified by the associated metric tensor. The metric tensors for a range of orientation spaces were obtained from their actions on line elements of the spaces.[20] In order to use the ODF as a density in the Euclidean sense, it should be scaled by the metric. This means that the volume fraction of a texture component should be evaluated by both its ODF and its discretized volume element in the representation space. Just as the discretization of Euler space needs a metric for the volume element, which is defined by $dg = d\varphi_1 \sin \Phi \, d\Phi \, d\varphi_2$, so Rodrigues' space needs a metric, $\sqrt{\det g_{ij}}$, which leads to a volume element, $dv = \sqrt{\det g_{ij}}\, dr^i dr^j dr^k$. The volumetric distortion associated with a Rodrigues' space is also discussed in other work.[21] Kumar and Dawson have used the finite-element discretization for ODF calculation and the fundamental region in Rodrigues' space.

In this study, using the standard distribution proposed by Matthies, various model textures have been generated (Section II–A) in Euler space. The volumes of the spherical texture components are calculated using the misorientation approach in Euler space (Section II–B). In addition, fiber textures such as those that occur from wire drawing or extrusion, *e.g.,* <111>, <110>, and <100>, can be calculated with the angle distance (angle between plane normals) approach in the unit triangle of the inverse pole figure (Section II–C). This measure of orientation distance is equivalent to distance on the surface of a sphere. The useful applications are shown in Section III for rolling and drawing textures.

II. THEORETICAL BACKGROUND

The orientation of a crystal coordinate K_B in regard to sample K_A can be characterized by three numbers combined in the symbol, $g = \{\varphi_1, \Phi, \varphi_2\}$, in the Bunge Euler angle definition or $g = \{\alpha, \beta, \gamma\}$ in the Matthies/Roe definition. The orientation space, Euler space, or G space contains every orientation *g,* which describes the transformation of K_A into K_B.[2,7] This space is finite,

$$g:[K_A \rightarrow K_B] \text{ or } g^{-1} = g^T:[K_B \rightarrow K_A].$$

$$G: 0 \le \varphi_1, \varphi_2 < 2\pi; \quad 0 \le \Phi \le \pi \quad (g = \{\varphi_1, \Phi, \varphi_2\}), \text{ in Bunge}$$

$$\text{or } G: 0 \le \alpha, \gamma < 2\pi; \quad 0 \le \beta \le \pi \quad (g = \{\alpha, \beta, \gamma\}), \text{ in Matthies/Roe} \qquad [1]$$

with the space element or volume element,

$$dg = d\varphi_1 \sin \Phi \, d\Phi \, d\varphi_2 \text{ or } dg = d\alpha \sin \beta \, d\beta \, d\gamma$$

$$\int_G dg = 8\pi^2 \qquad [2]$$

When the orientations of discrete points are known in a body with volume *V,* the ODF, $f(g)$, is given by

$$f(g) = \frac{dV(g)}{dg} \qquad [3]$$

In order to develop a method of calculating volume fractions that can be applied to standard data sets from texture analysis, Euler space can be discretized on a 5 by 5 by 5 deg grid. Such a discretization is commonly used to quantify preferred orientation in a material by specifying the intensity at each point on the grid.[22] The choice of

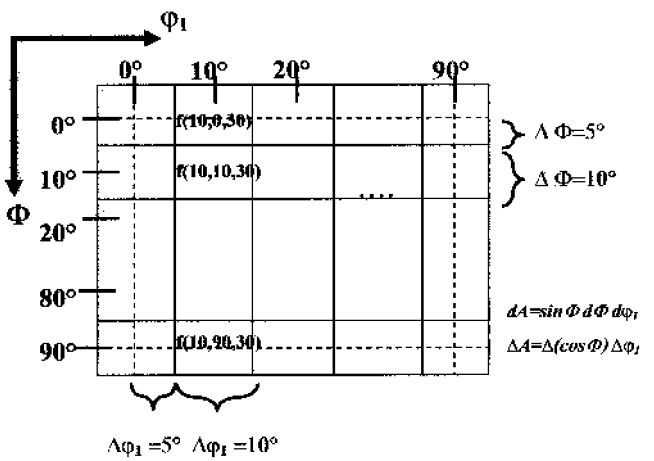

Fig. 1—Discrete ODF grid and centered cell structures. The end cells have different areas (φ_2 = 30 deg).

cell size determines the size of the volume increment, which depends on the value of the second Euler angle. The centered cell structure for a discrete ODF is shown in Figure 1, and the end cells have different areas. Euler angles are inherently spherical (globe analogy), and a Cartesian plot (orthogonal axes) of the ODF in Euler [angle] space has some distortions. Considering that the volume of Euler space is $8\pi^2$, a normalization is necessary. The summation of the discrete ODF over all the cells in Euler space should be unity.

$$1 = \frac{1}{8\pi^2}\sum_{\varphi_1}\sum_{\Phi}\sum_{\varphi_2} f(\varphi_1,\Phi_i,\varphi_2)\Delta\varphi_1\Delta\varphi_2 \left(\cos\left(\Phi_i - \frac{\Delta\Phi}{2}\right) - \cos\left(\Phi_i + \frac{\Delta\Phi}{2}\right)\right)$$

$$0 \le \varphi_1 \le 2\pi, 0 \le \Phi \le \pi, 0 \le \varphi_2 \le 2\pi \quad [4]$$

The volume fraction of a component of interest can be calculated by multiplication of the ODF by volume increment or invariant measure of each cell and summation of these products over the set of cells associated with the component.

A. *Standard Distributions*

The standard function is a useful model distribution for the ODF analysis.[7,8] In this study, the function is used for testing the calculation of volume fractions of spherical texture components using the misorientation angle in Euler space and fiber texture using the angle distance in the standard stereographic unit triangle. The intensity distribution of a texture component in a material is assumed to possess a bell-shaped structure, which can be described by a model distribution. Provided that the intensity distribution $f(b, g_0, g)$ has a texture component at g_0, it has the maximum value at g_0 and decreases with increasing orientation distance $\widetilde{\omega}(g_0, g)$. The expression for the orientation distance $\widetilde{\omega}$ between two orientations is

$$\widetilde{g} = g \cdot g_0^T = (g_0^T \cdot g)^T \quad [5]$$

$$\widetilde{\omega} = \widetilde{\omega}(g_0, g) = \widetilde{\omega}(g, g_0) \quad [6]$$

$$\cos\widetilde{\omega} = (\text{trace}(\widetilde{g}) - 1)/2 \quad [7]$$

The model distribution with half-width, b, is given by

$$f(b, g_0, g) = f(b, \widetilde{\omega}(g_0, g)) = f(b, \widetilde{\omega}) \quad [8]$$

$$\int_G f(b, g_0, g)\, dg = 16\pi \int_0^{\pi} f(b, \widetilde{\omega}) \sin^2(\widetilde{\omega}/2)\, d\widetilde{\omega} = 8\pi^2 \quad [9]$$

Two types of standard function can be used for texture modeling, *i.e.,* Gauss-shaped and Lorentz-shaped standard functions. A Gauss-shaped standard function, $f(S, \widetilde{\omega})$, is defined by

$$f(S, \widetilde{\omega}) = N(S)e^{S\cos\widetilde{\omega}} \ge 0,\ \widetilde{\omega} = \widetilde{\omega}(g_0, g),\ 0 \le S < \infty \quad [10]$$

For $S = 0$, Eq. [10] describes a random distribution, and for $S \to \infty$, it approaches the properties of the delta function, such as a single crystal. The function, $f(S, \widetilde{\omega})$, has its maximum at $\widetilde{\omega} = 0$ and its minimum at $\widetilde{\omega} = \pi$. The parameter S is given by a FWHM, b,

$$S = \ln 2/[2\sin^2(b/4)],\ b \le 2\pi \quad [11]$$

$$b = 4\arcsin(\sqrt{\ln 2(2S)}), S \ge \frac{1}{2}\ln 2 \approx 0.347 \quad [12]$$

The normalization constant $N(S)$ follows from Eq. [9] as

$$N(S) = [I_0(S) - I_1(S)]^{-1} \quad [13]$$

using the modified Bessel functions,

$$I_1(x) = \frac{1}{\pi}\int_0^{\pi} e^{x\cos t}\cos(lt)\, dt \quad [14]$$

The Bessel functions can be evaluated numerically.[23,24] This Gauss-shaped distribution is known to possess all the properties required of standard distributions.

The other standard function is the Lorentz-shaped standard distribution, which is

$$f(t, \widetilde{\omega}) \equiv (1 - t^2)\frac{(1 + t^2)^2 + 4t^2\cos^2(\widetilde{\omega}/2)}{[(1 + t^2)^2 - 4t^2\cos^2(\widetilde{\omega}/2)]^2} \quad [15]$$

For $t \to 0$, $f(t, \widetilde{\omega})$ describes a random distribution, and for $t \to 1$, it has the properties of a delta function at $\widetilde{\omega} = 0$. Although these two standard functions satisfy the general property of the orientation distance, $\widetilde{\omega} = \pi + \varepsilon \cong \pi - \varepsilon$, the Lorentzian distribution has a longer tail than the Gaussian distribution. The long tail of the Lorentzian function leads to a physically unreasonable coupling between the fitting near the maximum peak and in distant regions, which also contributes to an increase in the background. In addition to the maximum value at the peak, the integral intensity of the function has an important meaning for the components. The metric factor, $\sin^2(\widetilde{\omega}/2)$, of the Euler space related to ODF representation can exaggerate the differences between the distribution types.[25] The Gauss function has been found to be successful in eliminating ghost errors and allows for good fitting of typical multicomponent textures.[10] In this article, only the Gauss-shaped distribution is considered.

Model distributions were generated in the discretized Euler space with the standard accuracy for several texture components. Gaussian shape distributions, half-widths, background, crystal, and sample symmetry should be considered together. The model distribution, $f(g)$, must also have identical intensities at equivalent positions in Euler space with respect to both sample and crystal symmetries. From the sample and crystal symmetry.

$$f(g^{jk}) = f(g);\ g^{jk} \equiv g_{B_j} \cdot g \cdot g_{A_k}$$
$$g_{B_j} \in G_B;\ j = 1, 2, \ldots, N_B$$
$$g_{A_k} \in G_A;\ k = 1, 2, \ldots, N_A \quad [16]$$

where G_B and G_A are the proper rotation groups for crystal and sample symmetries, respectively, and g is written as an axis transformation or rotation matrix.[1,2] In the case of cubic crystal symmetry and orthorhombic sample symmetry, as in rolled cubic materials, $N_B = 24$ and $N_A = 4$. When the symmetry

properties are considered, the model ODF, $f^M(g)$, which has parameters I_n, b_n, g_0^n and background F, is given by

$$f^M(g) = F + \sum_{n=1}^{N} I_n \left\{ \left(\sum_{k=1}^{N_A} \sum_{j=1}^{N_B} f(b_n, \tilde{\omega}(g_{B_j} \cdot g_0^n \cdot g_{A_k}, g)) \right) / (N_A \cdot N_B) \right\} F + \sum_{n=1}^{N} I_n = 1 \quad [17]$$

where I_n is the volume of a given texture components at g_0^n and b_n is its half-width. The term N is the number of texture components. In what follows, all texture components are assumed to be spherical in shape, *i.e.,* varying in intensity only with distance (misorientation angle) away from the central location.

B. *Volume Fraction of Spherical Texture Components (Misorientation Approach in ODF Space)*

This section discusses volume collection of spherical texture components, and section C deals with fiber textures. The applications of spherical and fiber textures are shown in Sections III–A and B, respectively. Table I shows the intensities at the positions of standard textures components of spherical shapes with a Gaussian distribution. For simplicity, cubic/orthorhombic symmetry is assumed and the half-width of each component is fixed at 12.5 deg. All components have the same unit volume fraction (no background). Euler angles are given in both Bunge and Roe/Matthies angles. The multiplicity number, m, is also listed. The multiplicity number is related to the number of overlapped equivalent points of a component in Euler space. Cube and Goss have $m = 4$ and the highest ODF values, and brass and copper have $m = 2$. The S component has $m = 1$ and the lowest ODF value. The S component with $m = 1$ has 96 equivalent points in Euler space and none of the positions are overlapped, whereas the Goss component with $m = 4$ has 72 overlapped equivalent points among 96 points and only 24 points have unique positions. The multiplicity M_g of the orientation g is given by

$$M_g = \frac{N_A \cdot N_B}{N_{\text{uniq}}} \quad [18]$$

where N_A and N_B are given as the number of sample and crystal symmetry operators and N_{uniq} is the number of unique positions among the equivalent points. Note that the cube and rotated cube components share the characteristic of a "tube" of orientation along a line $\alpha + \gamma = const$ in Euler space, when β (or Φ) = 0. This characteristic is a consequence of the degeneracy of the Euler space at β (or Φ) = 0.

The presence of sample and crystal symmetry means that the ODF has equivalent positions in the Euler space. Cubic materials with orthorhombic sample symmetry have 96 equivalents points in the full Euler space. Even in the subspace used for the cubic/orthorhombic case (90 deg-90 deg-90 deg), there are three equivalent points for each component. The subspace can be readily separated to yield a fundamental zone (or asymmetric unit), but the shape of the resulting reduced subspace is inconvenient for graphical representation. Other orientation representation methods such as Rodrigues are preferred for this purpose.[26,27]

The misorientation analysis between grains or orientations has been extensively reviewed.[11,12] The orientation of a grain is represented as a rotation from sample coordinates K_A to crystal coordinates K_B. When two orientations are given as C_1 $[K_A \rightarrow K_B]$ and C_2 $[K_A \rightarrow K_B]$, and S_j describes one of the symmetry operations belonging to the appropriate crystal class concerned, the misorientation angle, θ, is given as

$$\theta = \min \left[\operatorname{acos} \left\{ \frac{\text{trace}\,((C_1 \cdot C_2^{-1}) \cdot S_j) - 1}{2} \right\} \right], \quad i = 1, \ldots, n;\ S_1 = E \quad [19]$$

The misorientation angle, θ, is the minimum value of angle distances among their equivalent orientations of two orientations with respect to crystal symmetry, while the orientation distance, $\tilde{\omega}$, is simply the angular distance between two orientations (Eqs. [5] through [7]). Figure 2 shows each of the texture components listed in Table I in the 90 × 90 × 90 deg subspace. The orientation number in Figure 2 corresponds to the orientation number in the footnote of Table II. Table II lists the misorientation angle and axis between some typical texture components, *i.e.,* brass, copper, *S,* Goss, and cube

Table I. Standard Texture of Spherical Components with Gaussian Distribution (b = 12.5 Deg) and Its Multiplicity (Cubic/Orthorhombic) in the 90 × 90 × 90 Deg Region

Miller Index {*hkl*}<*uvw*>	Euler Angles {φ_1, Φ, φ_2}	Euler Angles {α, β, γ}	ODF (Maximum at Exact Position)	Multiplicity (m)
Bs, {110}<112>	{35.26 deg, 45 deg, 0 deg}	{54.74 deg, 45 deg, 0 deg}	130.95	2
Copper, {112}<111>	{90 deg, 35.26 deg, 45 deg}	{0 deg, 35.26 deg, 45 deg}	130.95	2
S {123}<634>	{58.98 deg, 36.7 deg, 63.44 deg}	{31.02 deg, 36.7 deg, 26.57 deg}	56.89	1
Goss, {110}<001>	{0 deg, 45 deg, 0 deg}	{90 deg, 45 deg, 0 deg}	262.22	4
Cube, {001}<100>	{$\varphi_1 + \varphi_2$ = 0 deg, 90 deg, 180 deg, Φ = 0 deg}	{$\alpha + \gamma$ = 0 deg, 90 deg, 180 deg, β = 0 deg}	262.22	4
Rotated cube, {001}<110>	{$\varphi_1 + \varphi_2$ = 45 deg, 135 deg, Φ = 0 deg}	{$\alpha + \gamma$ = 45 deg, 135 deg, β = 0 deg}	262.22	4
Rotated Goss, {110}<011>	{90 deg, 45 deg, 0 deg}	{0 deg, 45 deg, 0 deg}	262.22	4
{111}<112>	{90 deg, 54.75 deg, 45 deg}	{0 deg, 54.74 deg, 45 deg}	130.95	2
{112}<110>	{0 deg, 35.26 deg, 45 deg}	{90 deg, 35.26 deg, 45 deg}	130.95	2

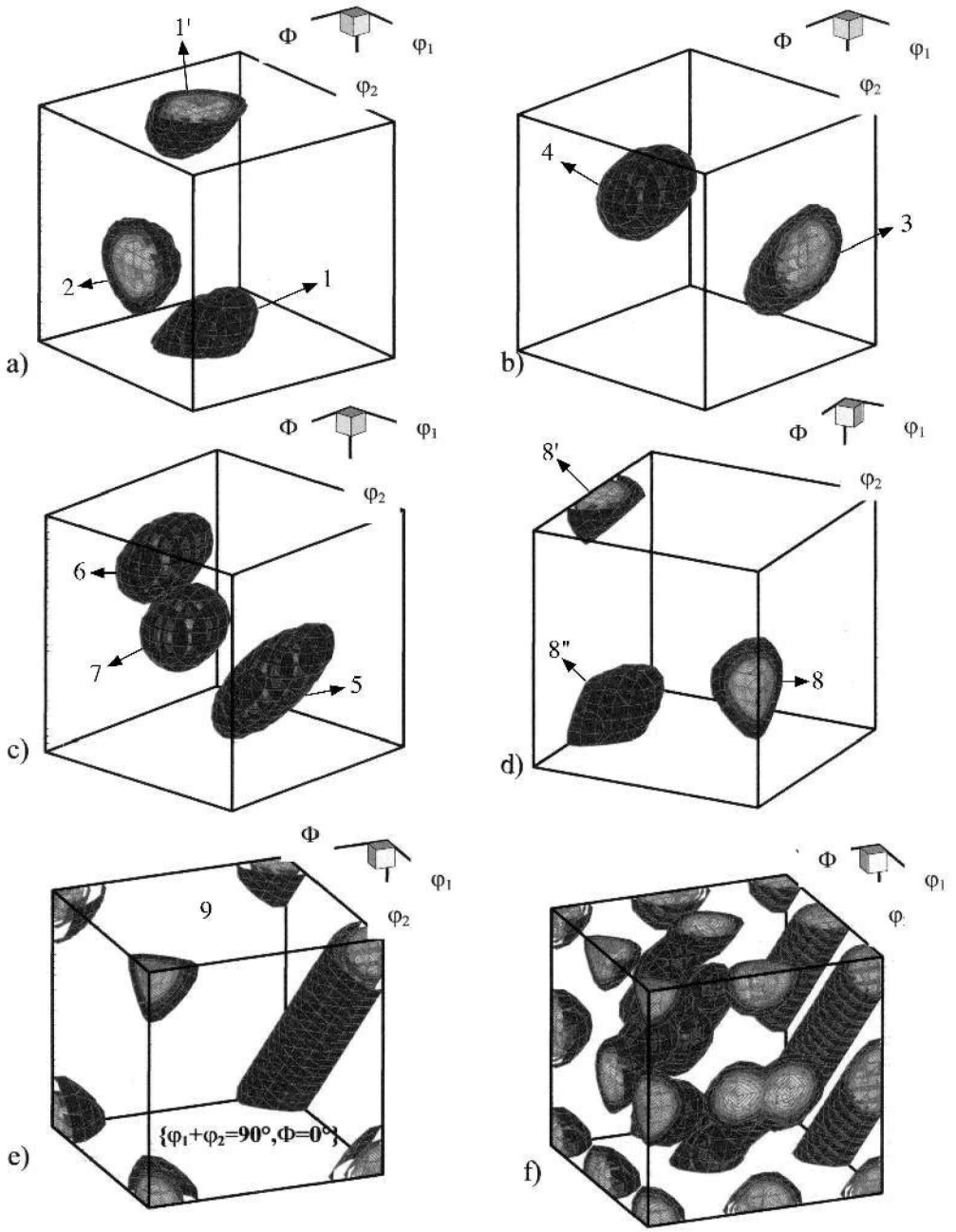

Fig. 2—Texture components generated by Gaussian distribution (b = 12.5 deg) in three-dimensional Euler space. The combined texture in (f) has the equal volume fractions of all nine components in Table I. The numbers have the following meanings: 1: {35.26, 45, 90} brass, 2: {54.74, 90, 45} brass, 3: {90, 35.26, 45} copper, 4: {39.23, 65.9, 26.57} copper, 5: {58.98, 36.7, 63.43} S, 6: {27.03, 57.69, 18.44} S, 7: {52.87, 74.49, 33.69} S, 8: {90, 90, 45} Goss, 9: {0, 0, 0} cube, 10: {45, 0, 0} rotated cube. (In this figure, the surface contour has unit ODF value and the center of a component has maximum ODF in Table I for each component.) (*a*) brass, (*b*) copper, (*c*) S, (*d*) Goss, (*e*) cube, and (*f*) combined texture.

and their physically equivalent points in the subspace. Although the brass component has three equivalent points in the subspace, orientation 1', {35.26 deg, 45 deg, 0 deg}, has no misorientation with 1, {35.26 deg, 45 deg, 90 deg}, because the two orientations are related by crystal symmetry only. This means that the two orientations are physically equivalent as well as equivalent in Euler space. The variants of the S component, which has multiplicity 1, exhibit a variety of misorientations between themselves; the misorientation angle/axis is 38.2 deg <1,1,1> between orientations 5 and 6 (Table II), 50.2 deg <43,64,64> between 5 and 7, and 38.6 deg <66,37,66> between 6 and 7. All three variants belong to the S component. The maximum possible misorientation angle in cubic materials is 62.8 deg and it occurs, for example, between the Goss, {90 deg, 90 deg, 45 deg}, and rotated cube, {45°, 0°, 0°}, components. A twin relationship (Σ3) occurs between the two brass variants or the two copper variants.

By considering these equivalent points, the Euler space can be partitioned between the various components of interest. If the dispersion in orientation about a component can be assumed to be spherical in misorientation angle, then the partitioning of

Table II. Misorientations between Typical Texture Components Expressed as Axis/Angle Pairs; the Numbers Represent Orientations*

	1	2	3	4	5	6	7	8	9	10
1		**60** <111>	35.6 <80 60 5>	35.6 <5 60 80>	19.4 <68 59 43>	19.4 <43 59 68>	53.7 <12 62 78>	35.3 <101>	56.6 <59 77 24>	46 <20 98 8>
2			35.6 <5 80 60>	35.6 <80 4 60>	53.7 <12 78 62>	53.7 <78 12 62>	19.4 <68 43 59>	35.3 <110>	56.6 <24 59 77>	46 <8 20 98>
3				**60** <111>	19.4 <72 60 35>	51.5 <76 57 35>	51.5 <57 76 31>	54.7 <110>	56.6 <24 59 77>	35.3 <110>
4					51.5 <57 31 76>	19.4 <60 35 72>	19.4 <72 35 60>	54.7 <101>	56.6 <59 77 25>	35.3 <101>
5						38.2 <111>	50.2 <43 64 64>	43 <82 37 45>	48.6 <52 56 64>	38.7 <33 89 31>
6							38.6 <66 37 66>	43.0 <37 45 82>	48.6 <56 64 52>	38.7 <89 31 33>
7								43 <82 45 37>	48.6 <52 64 56>	38.7 <33 31 89>
8									45 <001>	**62.8** <28 68 68>
9										45 <001>
10										

Note: Bunge notations
1: {35.26, 45, 90}, brass, 2: {54.74, 90, 45}, brass
3: {90, 35.26, 45}, copper, 4: {39.23, 65.9, 26.57}, copper
5: {58.98, 36.7, 63.43}, S, 6: {27.03, 57.69, 18.44}, S,
7: {52.87, 74.49, 33.69}, S, 8: {90, 90, 45}, Goss
9: {0, 0, 0}, cube, 10: {45, 0, 0}, rotated cube

Euler space is straightforward. Once the space has been partitioned, then the volume fraction of each component can be calculated easily. A cut-off or acceptance angle is chosen and all cells in the orientation distribution whose misorientation angle with respect to a particular component falls within the cut-off angle are included in the summation to obtain the volume fraction (Fig. 3(a)). Since the maximum possible misorientation angle is 62.8 deg, as noted previously, choice of a cut-off angle larger than this will yield unit volume fraction for a component. Figure 3(b) shows the relationship between three standard components, brass (number 1 in Table II), copper (number 3), and S (number 5). Certain combinations of orientations such as brass, copper, and S are too close together, however, because their collection volumes overlap. Since the misorientation between brass and S (number 5) is only 19.4 deg, it is clear that choosing a cut-off angle of 15 deg will result in appreciable overlap and thus double counting of the orientation distribution. The same situation exists between copper (number 3) and S (number 5). There are two solutions to this problem. One is to avoid using a cut-off angle larger than one-half of the smallest intercomponent misorientation in the chosen set of components. The second, employed here, is to partition the overlapped space so that those cells are assigned to the nearest component (provided that the cell is nearer than the cut-off angle to at least one component). Cells further away (in misorientation angle) than the cut-off are assigned to a texture category of "other" or "random."

C. *Volume Fraction of Fiber Texture Component (Angular Distance in an Inverse Pole Figure)*

Ideal fiber textures can be obtained by convoluting an orientation, g_0, with a cylindrical rotation symmetry element about an axis, n. The axis, n, of the fiber component is specified with respect to the sample coordinate system. If the starting distributions are given in $f(b, g_0, g)$, the corresponding fibers will be described by $f(b, n, g_0, g)$. In this case, g_0 has a different meaning because of the rotation around n and so it is taken as the mean of the rotation angle, $\overline{\varphi}$,

$$f(b, g_0, g) = f(b, n, g_0, g) \qquad [20]$$

$$g_0 \rightarrow g_0 \cdot \{n,0\}^{-1} \cdot \{n,\overline{\varphi}\}; \quad \int_0^{2\pi} d\overline{\varphi}/2\pi \qquad [21]$$

For the case of an ideal fiber texture, the intensity in the orientation distribution is identical for all orientations that are invariant with respect to the cylindrical symmetry element. In practical terms, a certain sample direction is aligned with the same crystal direction. An inverse pole figure map shows the distribution of a given sample direction with respect to crystal directions (in K_B). Therefore, it is useful to project the Euler space into a single unit triangle, (100-110-111), of an inverse pole figure (Figure 4) and plot intensities in, say, a stereographic projection. The standard stereographic triangle is the fundamental zone when a single direction is sufficient to describe orientation.

In general, the information in Euler space can be projected into an inverse pole figure map, $R_y(h_i)$, or a pole figure map, $P_{h_i}(y)$. Like the pole figure, an inverse pole figure also represents all crystallites orientated in such a manner that a direction h_i fixed and described in their crystal coordinate system K_B, and a sample direction y given in K_A, are parallel. For fixed h_i and y, $R_y(h_i)$ is proportional to the sum of all

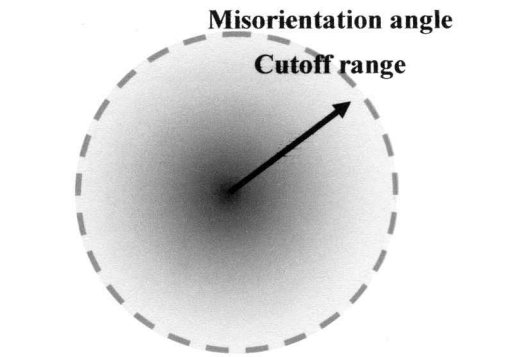

(*a*)

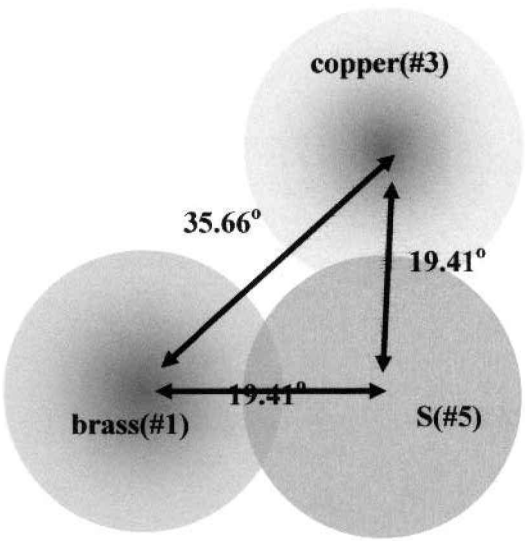

(*b*)

Fig. 3—Schematic diagrams considering the volume of the texture components. Figure (b) illustrates the potential for overlay between adjacent texture components: (*a*) texture distributions around ideal orientation and cut-off angle and (*b*) relationships between adjacent other components.

crystallites with the orientations g and frequency $f(g)$ meeting the condition y // h_i, *i.e.*, $h_i = g \cdot y$.[7]

$$P_{h_i}(y) = R_y(h_i) = \frac{1}{2\pi}\int_0^{2\pi} f(\{h_i,\overline{\varphi}\}^{-1} \cdot \{y,0\}\, d\overline{\varphi}$$

$$= \frac{1}{2\pi}\int_0^{2\pi} f(\{h_i,0\}^{-1} \cdot \{y,\overline{\varphi}\}\, d\overline{\varphi} \qquad [22]$$

The crystal direction h_i can be calculated directly from the orientation. The crystal direction, h_i, for a given fiber, *i.e.*, {111}, {110}, or {100}, is compared with the crystal directions of all orientations in Euler space, and the ODF, $f(g)$, for orientations within the cut-off angular distance is summed for the volume of that fiber. The angular distance between the crystal direction of the fiber component and a cell in the inverse pole figure is similar to the angular distance between two unit vectors $\mathbf{n_1}$ and $\mathbf{n_2}$. The angular distance $\zeta(0 \le \zeta \le \pi)$ between two unit vectors, $\mathbf{n_1}$ and $\mathbf{n_2}$, is given by the scalar product,

$$\mathbf{n_1} \cdot \mathbf{n_2} = \mathbf{n_1} \cdot \mathbf{n_2} = \cos\zeta \qquad [23]$$

The angular distance for fiber in the inverse pole figure is analogous to the misorientation angle for a spherically distributed component in Euler space. The angular distance is equivalent to a cut-off value between the ideal fiber line, or the skeleton fiber line and all orientations in Euler space. The skeleton fiber line defines an ideal fiber and orientations that deviate from the ideal fiber are included in the volume fraction for the fiber if they lie within the cut-off value.

III. APPLICATIONS

A. *Volume Fractions of Spherical Components*

The calculation of volume fractions was verified in Section II with the standard function combined with the Gaussian distribution. The verifications were made for two examples, a monocomponent (single-crystal) case and a multicomponent case (polycrystal).

1. *Single-crystal distribution*

The volume fraction of a single orientation is calculated in Euler space assuming a combination of cubic crystal and orthorhombic sample symmetry. A "standard ODF" is constructed for each ideal orientation, by calculating intensities for all cells in orientation space based on Eq. [17] and setting the background, F, equal to zero. The orientations considered are brass, S, copper, Goss, cube, rotated cube, rotated Goss, {111}<112>, {112}<110>, with b = 12.5 deg (in Table I). Some of them are shown in Figures 2(a) through (e). Each component is assigned a unit volume fraction and the expected volume should also be unity. Since it is assumed that a component has a bell-shaped distribution, there is some spread about its nominal position. After constructing each standard ODF, the volume fractions of the set of nine components are calculated by summing up the intensity of each cell in the ODF that lies within the cut-off misorientation value, 15 deg, of each component. The orientation space is partitioned, as described previously, in order to avoid overlaps and double counting. The result is shown in Figure 5. Generation of an ODF based on a single component with spread, b = 12.5 deg, leads to recovery of 90 pct of the volume fraction in the case of the brass, S, and copper components. The remaining 10 pct is assigned to other orientations because of overlaps between the collection volumes of each component. For the cube and Goss components, 95 pct of the original volume fraction is recovered.

2. *Polycrystal distributions*

In addition to the nine different single-crystal ODFs examined in Section III-A,1, three examples of polycrystal distributions were constructed. The same nine components in Table I were used, and the intensities in each cell from each component were added up and the resulting distribution normalized. The values of volume fraction and half-width for each component are given in Table III. Only the spread was varied between the three different ODFs with b = 7.5, 12.5, 20 deg, for cases 1, 2, and 3, respectively. Figure 2(f) shows the surface defined by an isointensity contour in Euler space for case 2, for which b = 12.5 deg.

Figure 6 shows the results of the volume fraction calculation. The Gaussian distribution with narrower half-width, b = 7.5 deg, leads to reasonable estimates of volume fractions

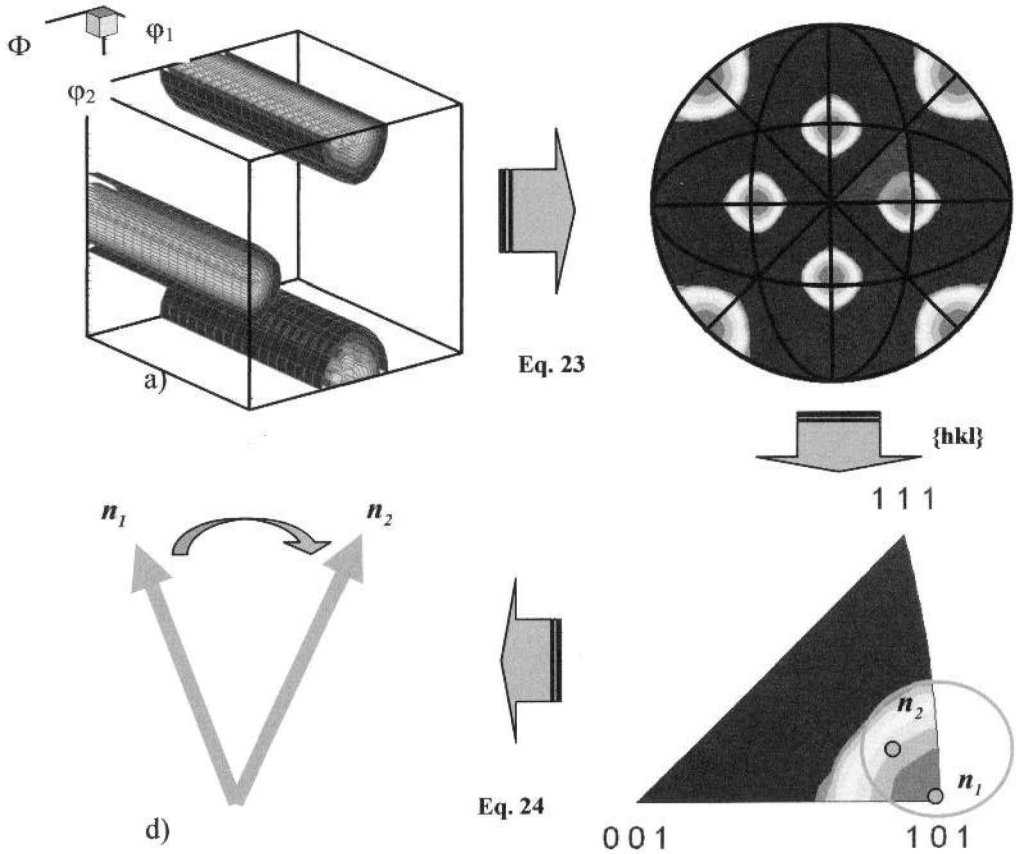

Fig. 4—Schematic drawing for reduction of Euler space *via* inverse pole figure to unit triangle. The angular distance $\zeta(0 \leq \zeta \leq \pi)$ is calculated with two direction vectors $\mathbf{n_1}$ and $\mathbf{n_2}$ in the unit triangle: (*a*) 110 fiber in Euler space, (*b*) ND inverse pole figure, (*c*) unit triangle for inverse pole figure, and (*d*) angular distance.

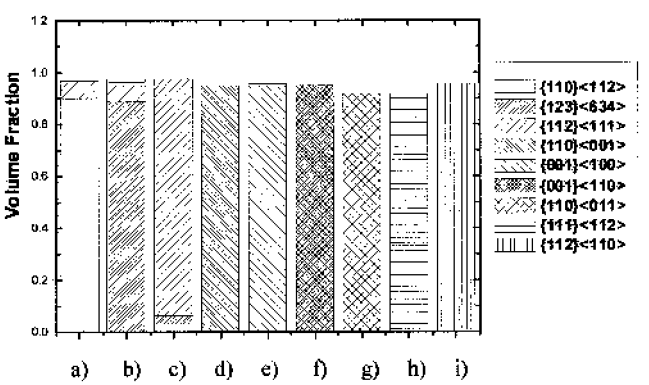

Fig. 5—Collected volume fraction of single orientation. Each component has unit volume in a Gaussian model distribution. The cut-off misorientation angle is 15 deg: (*a*) {110}<112>, (*b*) {123}<634>, (*c*) {112}<111>, (*d*) {110}<001>, (*e*) {001}<100>, (*f*) {001}<110>, (*g*) {110}<110>, (*h*) {111}<112>, and (*i*) {112}<110>.

for 10 and 15 deg cut offs (Figures 6(a) and (b)). For a distribution with half-width $b = 12.5$ deg, use of a 15 deg cut-off angle leads to reasonable volume fractions (Figure 6(d)): a narrower cut-off angle of 10 deg underestimates their volume fractions however (Figure 6(c)). For distributions with half-width $b = 20$ deg, both 10 and 15 deg cut-off values underestimate the volume fractions (Figures 6(e) and (f)).

B. *Volume Fractions of Fiber Components*

Table IV shows the volume fractions used to construct ODFs for each of the {111}, {110}, and {100} fiber textures (three cases) and an ODF with all three fibers combined. Each fiber had a Gaussian distribution, $b = 12.5$ deg. For the fourth case of the combined fibers, each of the {111}, {110}, and {100} fibers has an equal volume fraction, 0.333. Figure 7 shows isointensity surfaces for the {111}, {110}, and {100} fiber textures together with the combined fibers. With the angular distance approach and a cut-off angle of 15 deg, the collected volumes are 0.95, 0.95, and 0.95 for {111}, {110}, and {100}, respectively. For the case of the combined fibers, {111 + 110 + 100} and the same cut-off angle of 15 deg, the volume fractions of the three fiber components were 0.331, 0.325, and 0.325, respectively.

C. *Volume Fraction in Experimental Textures*

The two real examples for calculation of volume fractions are shown. One is for a cold-rolled copper sheet with intensity along both the alpha and beta fibers.[26] These are not fibers in the sense defined in Section II-C or III-B but do represent lines of intensity threading through orientation space along a series of typical orientations, {Goss~brass~S~copper}.[28] The beta fiber is represented approximately by the sequence brass-S-copper and the alpha fiber by the series of orientations between Goss and brass. The second example

Table III. The Volume and Half-Width for Mixed Nine Texture Components with Gaussian Distributions in Several Model Distributions Case

	Case 1		Case 2		Case 3	
Texture	Volume	FWHM(b)	Volume	FWHM(b)	Volume	FWHM(b)
Bs {110}<112>	0.11	7.5 deg	0.11	12.5 deg	0.11	20 deg
S {123}<634>	0.11	7.5 deg	0.11	12.5 deg	0.11	20 deg
Copper {112}<111>	0.11	7.5 deg	0.11	12.5 deg	0.11	20 deg
Goss {110}<001>	0.11	7.5 deg	0.11	12.5 deg	0.11	20 deg
Cube {001}<100>	0.11	7.5 deg	0.11	12.5 deg	0.11	20 deg
Rcube {001}<110>	0.11	7.5 deg	0.11	12.5 deg	0.11	20 deg
Rgoss {110}<011>	0.11	7.5 deg	0.11	12.5 deg	0.11	20 deg
{111}<112>	0.11	7.5 deg	0.11	12.5 deg	0.11	20 deg
{112}<110>	0.11	7.5 deg	0.11	12.5 deg	0.11	20 deg

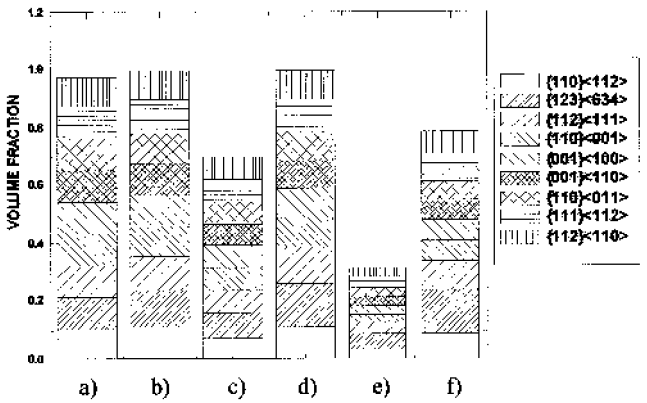

Fig. 6—Collected volume fractions of the ODF with nine texture components in Table III according to each cut-off value. b = 7.5 deg:(*a*) case 1 in Table III (cutoff 10 deg) (*b*) case 1 in Table III (cutoff 15 deg) b = 12.5 deg:(*c*) case 2 in Table III (cutoff 10 deg), (*d*) case 2 in Table III (cutoff 15 deg) b = 20.5 deg: (*e*) case 3 in Table III (cutoff 10 deg), (*f*) case 3 in Table III (cutoff 15 deg).

Table IV. The Original and Collected Volume for the Fibers Generated with Gaussian Distributions (FWHM, b = 12.5 Deg); the Cut-Off Value is 15 Deg

Fiber	Original Volume	Collected Volume
{111}	1	0.95
{110}	1	0.95
{100}	1	0.95
{111 + 110 + 100}	{0.333 + 0.333 + 0.333}	{0.331 + 0.325 + 0.325}

is measured for a gold bonding wire, which has very well developed {111} and {100} fibers.

1. *Cold-rolled copper (RA = 90 pct)*

The texture of a copper sheet cold rolled to a reduction in thickness of 96 pct was used. The measured texture has the well-known alpha and beta fibers and is shown as an isointensity contour map in Figure 8(a). Volume fractions for the nine components listed in Table I were calculated using the methods described previously and a cut-off angle of 15 deg. The elementary regions of Euler space were used to collect the volume of the texture components listed in Table I. The result shows that the strongest components in this rolling texture are S, brass, and copper. The brass and copper components have similar volume fractions and S has the maximum. The volume fraction of cube is similar to the copper component, whereas the Goss component is weaker than the cube component. The volume fractions of each of the components are affected by the choice of cut-off angle, as expected (Figure 9). The absolute values of the volume fractions increase with increasing cut-off angle, but the ratios between components are not changed.

2. *Gold wire drawing*

The texture of a gold bonding wire (diameter 30 μm) was measured with automated EBSD after drawing to an equivalent strain of 11.4. Using a cut-off angle of 15 deg, the volume fraction of the {111} fiber is 0.68 and the {100} fiber is 0.14, which gives a ratio of {100}/{111} = 0.20. The volume fraction of the {110} fiber was negligible. This result shows that the {111} fiber is dominant with respect to {100} during wire deformation of gold. This result is typical for drawing textures in medium and high stacking fault energy fcc metals. The volume fractions obtained depend on the cut-off angle chosen, but the largest volume fraction is always {111} (Figure 10). As the cut-off value increases, all the volume fractions increase as expected. The EBSD data were converted into an ODF using the WIMV method and isointensity maps are shown in Euler space (Figure 8(b)).

IV. SUMMARY

A rational method for determining volume fractions of texture components has been presented that is based on partitioning orientation space using the misorientation angle as a measure of distance in orientation space. This approach has been verified by first generating idealized discrete orientation distributions in Euler space for single-component and poly-component textures using a modified (spherical) Gaussian distribution and then applying the partitioning approach to calculate volume fractions.

1. Texture components can be modeled with standard Gaussian function or Lorentzian functions. Examples of spherical and fiber components in Euler space have been modeled with the Gaussian function for verification of volume fraction calculations.
2. Texture components have different multiplicities depending on their location with respect to symmetry elements. The S component has multiplicity 1 and brass and copper

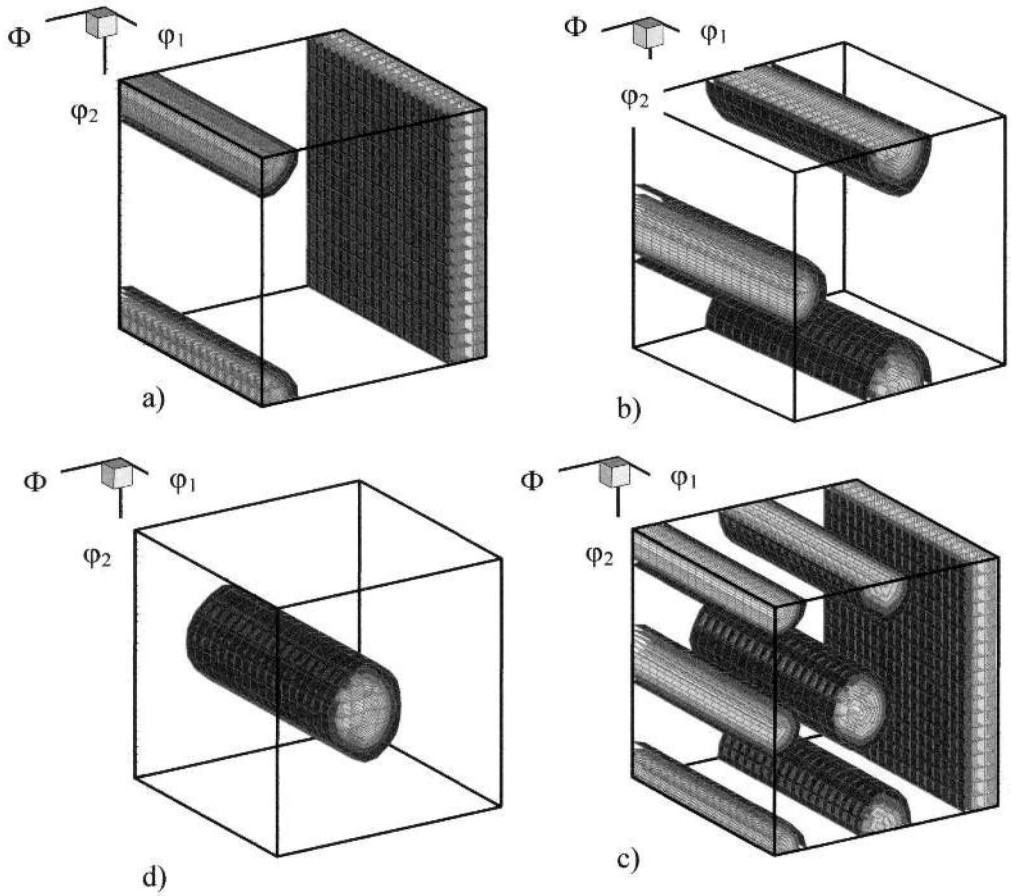

Fig. 7—Fibers generated by Gaussian distribution (b = 12.5 deg) in three-dimenstional Euler space: (a) {100}, (b) {110}, (c) {111}, and (d) {111 + 110 + 100}.

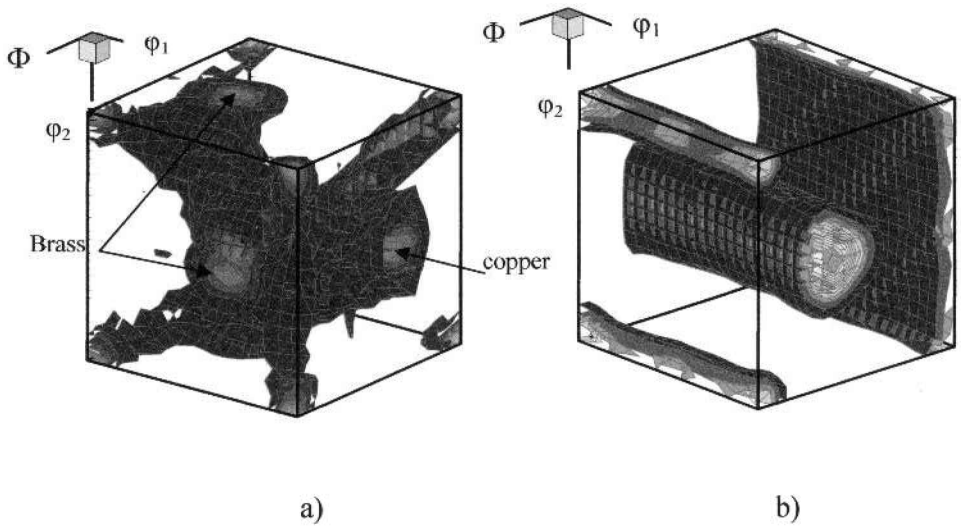

Fig. 8—ODF for deformed metals: (a) cold-rolled copper (RA = 96 pct) and (b) cold-drawn gold bonding wire (ε_{eq} = 11.4).

have 2. The high symmetry orientations, Goss and cube, have multiplicity 4.

3. The misorientation angle between pairs of orientations can be used as a measure of distance in Euler space in order to partition the space among a set of discrete components. Once the space has been partitioned, volume fractions can be calculated in a straightforward manner either by integrating continuous functions or summing intensities in discrete distributions.
4. The volume fractions of fiber texture components can be collected using the interplanar angle distance approach to partition a distribution of sample directions. For cubic

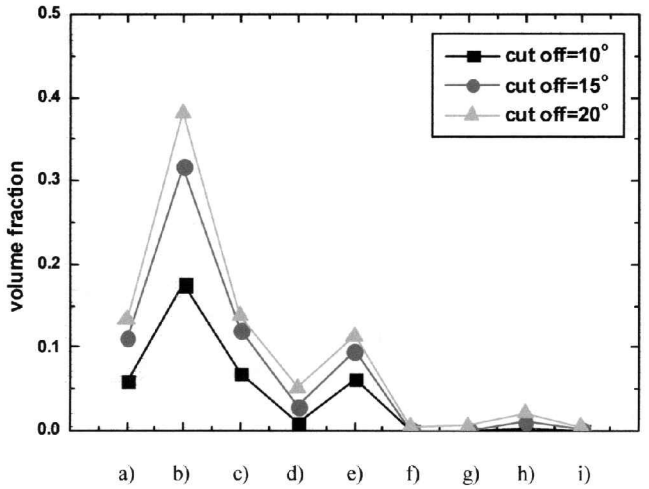

Fig. 9—The volume of texture components in cold-rolled copper. The volume fractions are variable according to cut-off value. (*a*) brass, {110}<112>; (*b*) S, {123}<634>; (*c*) copper, {112}<111>; (*d*) Goss, {110}<001>; (*e*) cube, {001}<100>; (*f*) rotated cube, {001}<110>; (*g*) rotated Goss, {110}<011>; (*h*) {111}<112>; and (*i*) {112}<110>.

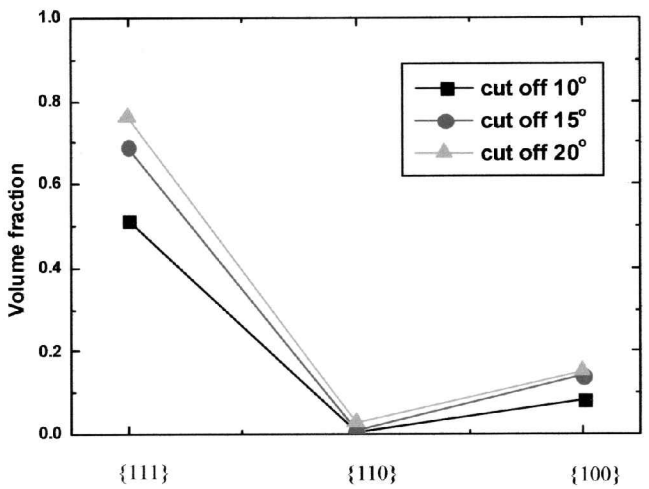

Fig. 10—The volume of fiber texture components in gold wire. The volume fractions are variable according to cut-off value.

materials, the partitioning can be performed in the fundamental zone (asymmetric unit) of the 001-110-111 unit triangle of an inverse pole figure.

5. Volume fractions calculated in this way are reasonable for experimental textures measured in metals.

ACKNOWLEDGMENTS

This research is supported by the BK21 project of the Ministry of Education & Human Resources Development, Korea. This work was also supported in part by the MRSEC program of the National Science Foundation under Award No. DMR-0079996. J.H. Cho is particularly grateful to Dr. S. Matthies for his advice and guidance.

APPENDIX

The working steps for partitioning of cell-structured Euler space (cubic crystal/orthorhombic sample case) are as follows.

Step 1. Identify the equivalent points of a texture component of interest in Euler space (*i.e.*, 90 deg-90 deg-90 deg).

$$g_{ij}^0 = S_{ik}^c \cdot g_{kl}^0 \cdot S_{lj}^s$$

$$g_{ij}^0 = \{\alpha, \beta, \gamma\} \text{ or } \{\varphi_1, \Phi, \varphi_2\}, \text{ all components} \leq 90 \text{ deg}$$

S^c: crystal symmetry operator, S^s: sample symmetry operator.

Step 2. Calculate the misorientations between the equivalent points in step 1 and each cell in the discretized Euler space.

$$\theta = \min \left[\text{acos} \left\{ \frac{\text{trace}\,(S^c \cdot (g^0 \cdot g_{\{\alpha,\beta,\gamma\}})) - 1}{2} \right\} \right],$$
$$\alpha,\beta,\gamma{:}0 \text{ to } 90 \text{ deg (in 5 deg step)}$$

Step 3. Partitioning of the Euler space.

$$\text{If } (\theta \leq \text{acceptance angle}), \text{ then } g^0 = g_{\{\alpha,\beta,\gamma\}}$$

Step 4. Compare the misorientation angles in step 3 among the list of texture components.

For a given cell, the specific texture component with the minimum misorientation angle from step 3 is assigned the intensity of that cell.

REFERENCES

1. H.J. Bunge: *Texture Analysis in Materials Science,* Butterworth and Co., London, 1982.
2. H.J. Bunge and C. Esling, (Hrsg.): *Quantitative Texture Analysis,* DGM Informationsgesellschaft, Oberursel, 1982.
3. H.R. Wenk: *Preferred Orientation in Deformed Metals and Rocks: An Introduction to Modern Texture Analysis,* Academic Press, San Diego, CA, 1985.
4. S. Matthies and G.W. Vinel: *Phys. Status Solidi,* 1982, (b) 112, pp. K111-K114.
5. U.F. Kocks, C.N. Tomé, and H.-R. Wenk: *Texture and Anisotropy,* Cambridge, University Press, Cambridge, United Kingdom, 1998.
6. H.J. Bunge: *Mathematische Methoden der Texturanalyse,* Akademie-Verlag, Berlin, 1969.
7. S. Matthies, G.W. Vinel, and K. Helming: *Standard Distributions in Texture Analysis,* Akademie-Verlag, Berlin, 1987.
8. S. Matthies: *Phys. Status Solidi,* 1980, (b) 101, pp. K111-K115.
9. J. Hirsch and K. Lücke: *Acta Metall.,* 1988, vol. 36 (11), pp. 2863-82.
10. K. Lücke, J. Pospiech, J. Jura, and J. Hirsch: *Z. Metallkd.,* 1986, vol. 77, pp. 312-21.
11. V. Randle and O. Engler: *Introduction to texture analysis*: *macrotexture, microtexture and orientation mapping,* Gordon & Breach Science Publishers Amsterdam, 2000.
12. V. Randle: *The Measurement of Grain Boundary Geometry,* Institute of Physics Publishing, UK, 1993, chs. 2-3.
13. J.K. Mackenzie: *Biometrika,* 1958, vol. 45, pp. 229-40.
14. D.C. Handscomb: *Can. J. Math.,* 1958, vol. 10, pp. 85-88.
15. A. Morawiec: *Acta Cryst.,* 1997, vol. A53, pp. 273-85.
16. K. Rajan and R. Petkie: *Mater. Sci. Eng.,* 1998, vol. A257, pp. 185-197.
17. N.R. Barton and R.R. Dawson: *Metall. Trans. A,* 2001, vol. 32A, pp. 1967-75.
18. C. Niels, L. Krieger, and D.J. Jensen: *Acta Cryst.,* 1994, vol. A50, pp. 741-48.
19. K. Kunze, S.L. Wright, B.L. Adams, and D.J. Dingley: *Textures Microstr.,* 1993, 20 (1–4), pp. 41-54.

20. A. Morawiec: *J. Appl. Cryst.,* 1990, vol. 23, pp. 374-77.
21. A. Kumar and P.R. Dawson: *Computational Mechanics,* 1995, vol. 17, pp. 10-25.
22. J.S. Kallend, U.F. Kocks, A.D. Rollett, and H.-R. Wenk: *Mater. Sci. Eng.,* 1991, vol. A132, pp. 1-11.
23. M. Abramowitz and I.A. Stegun: *Handbook of Mathematical Functions with Formulas, Graphs, and Mathematical Tables,* National Bureau of Standards, US Government Printing Office, Washington, DC, 1964.
24. G.N. Watson: *A Treatise on the Theory of Bessel Functions,* University Press, Cambridge, United Kingdom, 1945.
25. S. Matthies: *Phys. Status Solidi,* 1982, (b) 112, pp. 705-16.
26. F.C. Frank: *Proc. ICOTOM-8,* TMS, Warrendale, PA, 1988, pp. 3-13.
27. A. Heinz and P. Neumann: *Acta Cryst.,* 1991, vol. A47, pp. 780-89.
28. U.F. Kocks, C.N. Tomé, and H.-R. Wenk: *Texture and Anisotropy,* Cambridge University Press, Cambridge, United Kingdom, 1998, pp. 181-91.